METHODOLOGY AND CHARACTERIZATION OF PHOTO-POLYMERIZATION PROCESS USING UV CURABLE RESIN

by

SHAHID FAIZEE

Presented to the faculty of the Graduate School of

The University of Texas at Arlington in Partial Fulfilment

of the Requirements

for the Degree of

MASTER OF SCIENCE IN MECHANICAL ENGINEERING

THE UNIVERSITY OF TEXAS AT ARLINGTON

December 2015

ACKNOWLEDGMENTS

I would like to take this opportunity to thank my principal advisor Dr. Panayiotis S. Shiakolas for his guidance and support throughout my graduate research work. I would also like to thank my graduate committee members Dr. Pranesh Aswath and Dr. Tre Welch for their interest and advice.

I would like to thank my colleagues at the Micro Manufacturing Medical Automation and Robotics Systems (MARS) laboratory including Prashanth Ravi, Tushar Saini, Christopher Abrego, Shashank Kumat, Vishal Sarode, Md Abu Hasan, Michael Sobhy, Pradeep Mohan, Utsav Shah, Mayank Patel for their ideas and support throughout my work.

I would also like to thank Dr. Moon from the department of Mechanical and Aerospace Engineering for providing access to Nikon Microscope for my research work.

I would also like to thank the Fabrication Lab (FabLab) at University of Texas at Arlington Libraries for allowing the use of their equipment in the fabricating of required prototype models for my research work and the MAE machine shop personnel Mr. Kermit Beird and Mr. Sam Williams for their help with equipment fabrication.

November 17, 2015

ABSTRACT

METHODOLOGY AND CHARACTERIZATION OF PHOTO-POLYMERIZATION PROCESS USING UV CURABLE RESIN

Shahid Faizee, MS

The University of Texas at Arlington, 2015

Supervising Professor: Panayiotis S. Shiakolas

Photo-Polymerization (PP) based Additive Manufacturing (AM) technology, also known as Stereolithography (SLA), Rapid Prototyping, or Resin Printing, is very popular technique in 3D printing (3DP) applications. It offers a great advantage over the most common type of 3D printing technique called Fused Filament Fabrication (FFF) in terms of resolution, because resolution in SLA or PP is primarily determined by the spot size of the ultraviolet (UV) source and has a better surface finish due to reduce required force in the layer formation in comparison with FFF. In this research work, the PP module of the multi-modality BioPrinter was developed and the process was characterized using UV light and Solarez 3D printing resin. The process parameters considered in the characterization experiments were nozzle-to-bed distance, nozzle diameter, print head speed and power of the UV Light Emitting Diodes (LEDs). The effects of resin viscosity and resin feed value on the process were also studied. The resin viscosity plays a major role in influencing the dimensional stability of the polymer resin and affects the geometry and the cross-section of the strand fabricated. The characterization experiments for the PP process based on the partial Design of Experiment (DOE) using Design Expert Software from Stat-Ease® were performed assuming cylindrical profile for the strands fabricated. The width (response data) of the strand were found to 3-4 times the nozzle diameter due to the low viscosity of the Solarez resin used. In this work,

the viscosity of the Solarez resin was increased by freezing the resin in a conventional freezer. The rationale was to improve the dimensional stability of the resin for stable filament extrusion and thus perform the characterization experiments. The feed for the characterization experiments should also be adjusted based on the observed segment of a circle profile rather than the assumed cylindrical profile. Also, it is recommended to use a high molecular weight resin to minimize the effect of viscosity on the geometry of the fabricated strands.

TABLE OF CONTENTS

LIST OF ILLUSTRATIONS

LIST OF TABLES

CHAPTER 1

INTRODUCTION

1.1 Introduction to Additive Manufacturing (AM) and 3D printing

The cost of using metal fabricated components for experimental purposes can be costly due to multiple iterations prior to fabrication of final product. The discovery of fabricating a 3D object using a technology called Additive Manufacturing (AM) has proved to be an evolutionary process with the early AM equipment and materials developed in 1980s [1]. AM is a layer by layer fabrication technology to produce a 3D object also called 3D printing.

The general principles or steps for fabricating a solid model through 3D printing are as follows:

1. Modelling: The 3D object to be fabricated is first designed in a CAD (or 3D modelling) software and then converted to STL or OBJ format, a compatible file format suitable for most of the available commercial and personal 3D printers.
2. Printing: After converting the desired 3D model to STL or OBJ file, it is checked for manifold or water tight error and is fixed using appropriate software such as Netfabb before it is finally converted or sliced to G-code. Slicing is the process of converting the 3D model to a number of layers according to the specified layer height, infill density, print head speed, wall thickness, and raft and support material. After slicing the 3D model in the desired slicing software, the generated G-code is uploaded to a 3D printing client. There are various 3D printing clients available in the market such as Repetier, Pronterface, Matter Control, etc. Commercial 3D printer manufacturers such as Stratasys, 3D Systems, Envisiontec, and Makerbot have their own closed source software that is used to run only on their 3D printers.

3. Finishing: After the 3D object is fabricated, the surface finishing process of the 3D object can be performed using acetone, isopropyl alcohol and can even be painted. Some of the 3D objects require support material to be printed due to their complex structure. Some 3D printers such as Uprint have support structures that can be easily removed by mechanical or chemical method such as sodium hydroxide (NaOH) solution.

1.1.1 Review of Additive Manufacturing

In 1981, Hideo Kodama of Nagoya Municipal Industrial Research (NMIR) discovered a method for printing a 3D object using polymer that hardens when it is exposed to UV light and was controlled by mask pattern or scanning fiber transmitter [1]. A mask pattern is a mechanism in which the area which is desired to be photo hardened is exposed to UV light and the rest of area is covered to prevent any exposure to UV radiation. A scanning fibre transmitter is a device used to harden the liquid polymer resin by using an optical fibre mounted on XY plotter and controlling the scanning speed and exposure area [2]. Chuck Hull of 3D Systems Corporation, in 1984 invented a technique based on stereolithography, in which layers of photo-polymerized strand are constructed one on top of other by curing a polymer resin (monomers + photo-initiator) with UV laser(s) [3]. The resulting thickness of the substrate is a function of UV light intensity and the exposure time. As the UV light intensity and exposure time increase, the polymer cross linking density increases throughout the polymer thickness. Hull's contribution was in the design of a specific file format which is acceptable by most of the 3D printers around the globe for the purpose of fabricating 3D objects and was coined the term "STL" (STereoLithography) [3]. There are variety of materials that can be used with different technologies available for 3D printing such as plastic filaments that include ABS (Acrylonitrile Butadiene Styrene), PLA (Polylactic Acid), nylon, and T-glass, polymer resins such as Solarez resin, NEA123T, UV150DC and various other photopolymers, as well as metals such as steel, titanium, sliver, etc.

Table 1.1 discuss the main historical achievements in AM industries from 1987 to 2013. See Appendix B for further details.

Table 1.1 Chronological Order of Additive Manufacturing [4]

Date	Achievement	Name of the Achiever
1987	Development of Stereolithography (SLA)	3D Systems
1991	Invention of Fused Deposition Modelling (FDM)	Stratasys
1992	Selective Laser Sintering (SLS)	DTM (now a part of 3D Systems)
2012	Introduced laser- based vat Photo-Polymerization system	Formlabs
2012	Launch of first 3D bio-printing software	Orgonovo Holdings and Autodesk
2012	Development of two photon lithography for printing 3D object with fine details	Vienna University of Technology
2013	Development of laser 3D printing with maximum processing size of 1.8m	Dalian University of Technology and Unit Science and Technology Co. Ltd.

Table 1.1 Continued

2013	Development of Peachy Printer, world's first $100 3D printer	Rylan Grayson
2013	Development of low cost 3D metal printer	Michigan Technological University
2013	Launch of CLIP (Continuous Liquid Interface Production) Technology based on photo-polymerization	Carbon3D

1.1.2 Different Methods of Additive Manufacturing

There are various methods of fabricating 3D objects using AM technology.

1. Stereolithography [3]: This is the process of curing liquid or uncured polymer using a laser or UV LEDs. In this process, a vat with an attached build platform inside is filled with uncured polymer resin and as the UV laser is fired to polymerize the layer of desired height, the build platform moves a step down through a plunger attached to the build platform. This step corresponds to the layer height. The stereolithography process then continues with the build platform moving a step down (according to the specified layer height) after each layer has solidified.

2. Fused Deposition Modelling (FDM) or Fused Filament Fabrication (FFF) [5]: The 3D objects are fabricated layer by layer using the extrusion of molten plastic with layer heights ranging from 0.01 to 0.016in [6]. The extruder is heated to a temperature between 190°C and 260°C depending upon the type of polymer used such as Polylactic acid (PLA), Acrylonitrile Butadiene

Styrene (ABS), nylon, etc. The glass transition and the processing temperature of the 3D printing polymers are given in Table 1.2.

Table 1.2 Glass transition and processing temperature of 3D printing plastics [7]

3D printing plastic	Glass transition temperature	Processing temperature
Polylactide (PLA)	60-65 ℃	180-220 ℃
Acrylonitrile Butadiene Styrene (ABS)	105℃	210 - 260℃
Nylon	70℃	225-260℃
PETT "T-glase"	78℃	212-224℃
PVA (Polyvinyl Alcohol)	85℃	210-225℃

3. Material Jetting [6]: In this technique, a layer of uncured polymer resin is sprayed onto the build platform and UV treatment is then applied to cure the polymer.

4. Binder Jetting [6]: A layer of binder material is applied onto a layer of powdered material and then cured. The layers are post processed to remove the binder material. The post processing of the binder is performed by infiltration or bakeout.

5. Selective Laser Sintering (SLS) [6]: A laser is used to sinter or in simple words bind the powered material selectively by melting the particles at the surface. In this process, UV laser selectively fuses a layer of powdered material dispersed on the build platform. After the initial

layer is constructed, the bed lowers down through a plunger attached, similar to SLA process. A roller is then used to evenly spread the powdered material onto the build platform. Similarly, the successive layers continue to build until the final product is fabricated.

6. Sheet Lamination [6]: In this technique, a layer of adhesive is deposited according the desired shape onto a sheet of paper. Then a second paper is the placed on the adhesive and a presser is used to compress the adhesive sandwiched between the two sheets of paper. An adjustable carbide blade is used to cut the paper by tracing the outline of the layer. The process then continues until the 3D object is completely fabricated.

7. Syringe or Viscous Extrusion (VE) [6]: Syringe or Viscous Extrusion is used in a variety of 3D printing application such as photo polymerization.

1.2 Introduction to Photo-Polymerization (PP)

Photo-Polymerization is a process of converting a combination of binders and monomer in the form of a gel into a solid component by mixing a photo-initiator with the polymer and using a UV light source such as UV LEDs, and laser(s) for the solidification process.

Photo-Polymers consist of three main ingredients: binders or oligomers, monomers and photo-initiator. “The binders or oligomers constitute 50-80% of the weight of the photopolymer” [8]. Binders are also responsible for giving the final hardened polymer its mechanical properties. “Monomers are small molecules which are present in the polymer resin and constitute 10-40% weight of the resin”. They are also responsible for lowering the viscosity of the solution formed from binders [8]. The photo-initiator is substance which is mixed with monomer and oligomers and initiates the cross linking process called curing, when exposed to UV light. Photo-initiators are substances that decompose into radicals when exposed to UV or visible light and activates or initiates the photo-polymerization process [8]. The UV light is preferred over visible light because UV light is more energetic and initiates the Photo Polymerization faster than visible light [8].

The Photo-Polymerization process is pictorially represented in Figure 1.1

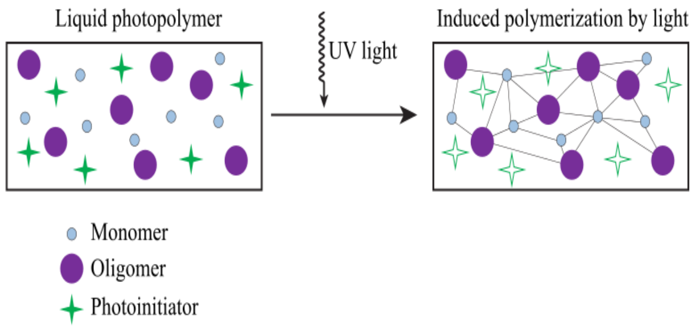

Figure 1.1 Photo-Polymerization Chemical Reaction Consisting of Monomers, Oligomers and Photo-initiators [9]

1.2.1 Free Radical Reactions

Free radical reactions occur when photo-initiators are dissociated when exposed to light forming free radicals. The free radical induce cross linking reaction of mixture of oligomers and monomers to form a cured film [10]. Free radical reactions occur with photo-initiation, chain propagation and chain termination [11].

1.2.2 Ionic Reactions

Ionic reactions occur when, an ionic photo-initiator is used to activate the Photo-Polymerization process through cross linking. Here the monomer is doped with either cationic or anionic photo-initiator that will initiate the curing process when radiated with light. Monomers which are used for cationic photo-polymerization includes styrene compounds, vinyl ethers, and lactones. There are several kinds of cationic photo-initiators available such as onium salts, organometallic compounds, and pyridinium salts [12]. The cationic Photo-Polymerization is more popular than anionic Photo-Polymerization as it is still under investigation [12]. One of the disadvantages of using photo-initiators is that they operate at a short range of UV wavelength between 320-395 nm [13].

1.3 Photo-Polymerization and 3D Printing

Photo-Polymerization was the first technology to be developed among the different technologies available for 3D printing such as Fused Deposition Modelling (FDM), Selective Laser Sintering (SLS), sheet lamination, and binding of granulated materials [6]. In the early stages of Photo-Polymerization process, a vat of liquid resin was exposed to a controlled UV light through a laser beam under safelight conditions [14]. As the UV light falls on the initial layer of the liquid resin, it solidifies the resin. After the initial layer is solidified, the build plate moves down according to the layer height specified and continues to build the desired object. The downward motion of the build platform is made through the use of a piston. The laser beam scans the layer under consideration and fuses the uncured resin selectively based on the desired 3D product. After the desired object is fabricated, the rest of the liquid polymer is drained and can be reused. The SLA process using a laser beam is represented in Figure 1.2.

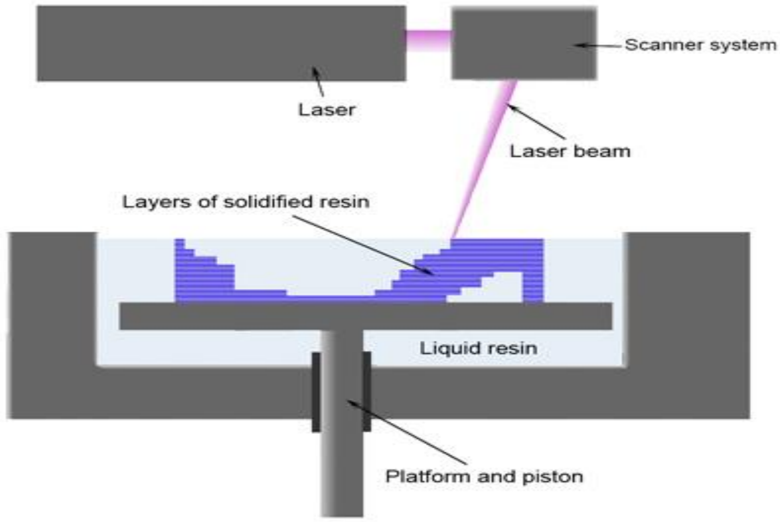

Figure 1.2 Stereolithography apparatus showing the polymerization of uncured resin using UV Light Source [14]

With Photo-Polymerization in 3D printing, the desired resolution can be as precise as 50 microns as compared to Fused Deposition Modelling (FDM) technique which has resolution of as low as 125 microns. The better resolution in Photo-Polymerization process is due to the spot size of the UV source. Also, PP has better surface finish due lower amount of force applied on the layer when compared to FFF method [15]. Due to small spot size of the UV source, the tolerance for a 3D object fabricated using PP method is between 50-125 microns [6].

1.4 Current Research Objectives

The objective of this research is to design a Viscous Extrusion (VE) or Photo-Polymerization (PP) module for the multimodality 3D BioPrinter and to study the effects of the combination of the process parameters on the characteristics of the fabricated strands. The research objectives also include the study of the effects of viscosity on the characterization of the Solarez 3D printing resin.

The process parameters considered are the feed (the rate at which the plunger moves), print head speed (the translational speed that the printer moves), nozzle-to-bed distance and the intensity or power of the UV light. The cross-section of fabricated strands are characterized using a Nikon microscope [16] (Nikon, Eclipse, USA).

The PP module consists of an LED fixture plate for attaching the UV LEDs at combination of desired angles and distance from the syringe nozzle for the PP process. The LED angle with respect to the syringe nozzle should be set such that there is no clogging of the nozzle due to the incidence of UV light on the syringe nozzle. Also the distance of the LED from the syringe nozzle should be such that the extruded uncured resin should be solidified all the way through.

Analysis and discussion on the methods of increasing the viscosity of the low viscous resin are studied in order to improve the dimensional stability of the low viscosity based Solarez 3D printing resin.

1.5 Outline of Thesis

Chapter 1 provided an introduction to AM and 3D printing and discussed a brief history on AM Technology called Stereolithography (SLA). It also discussed the various PP reactions and introduced the PP technology in 3D printing. The objectives related to the current research work were also discussed.

Chapter 2 discusses the Introduction to Manufacturing Automation and Robotics Systems (MARS) Lab BioPrinter and gives an overview of the different types of AM modules incorporated on it. It also discusses the slicer software and the features associated with it for assigning the various properties such as infill density, layer height, and speed of the print head for printing the

3D object. The 3D printing clients – Repetier is also discussed in this chapter. An introduction to the Marlin firmware and the RUMBA control board is also given.

Chapter 3 discusses the PP module setup including the various components associated. It also discusses about the 3D printing resin, the UV LEDs used, the power supply to control the power of UV LEDs, and the stepper motor used to dispense the 3D printing resin.

Chapter 4 discusses the characterization experiments conducted using the Solarez 3D printing resin in the PP module. It describes the various process parameters affecting the characterization of the Solarez resin and discusses the effects of viscosity on the characterization process as well as the method of increasing the viscosity of the resin to improve its dimensional stability.

Chapter 5 summarizes the characterization test runs performed and their results. It lists the conclusion of the current research work. It also gives a brief introduction on future work that can be performed to characterize a 3D printing resin using the PP module.

The introduction to PP was discussed in this chapter which will form the basis for the characterization of the Solarez resin based on the process parameters defined. This chapter also gave a brief review of AM outlining historical achievements made in the industry of 3D printing. The multimodality BioPrinter with different modules such as Fused Filament Fabrication (FFF), Photo-Polymerization (PP) and Inkjet (IJ) module will be discussed in the next chapter.

CHAPTER 2

MULTI-MODALITIY 3D BIOPRINTER

2.1 Multi-Modality BioPrinter

The custom multi-modality BioPrinter (CMMB) consists of a number of 3D printing modules on a single printing platform. The multimodality BioPrinter is under development at the Manufacturing Automation and Robotics Systems (MARS) research laboratory (http://mars.uta.edu) at the University of Texas at Arlington. This BioPrinter has a number of features including maximum print head speed of 600mm/min (10mm/sec), a double shaft stepper motor to control the Fused Filament Fabrication (FFF) modules, capability of housing up to five modules of different AM technologies, the RUMBA board used for extruder, motor and temperature control.

The CMMB is equipped with the following modules: Two Fused Filament Fabrication (FFF) modules, Photo-Polymerization (PP) module, Viscous Extrusion (VE) and an Inkjet Module. The CMMB is shown in Figure 2.1.

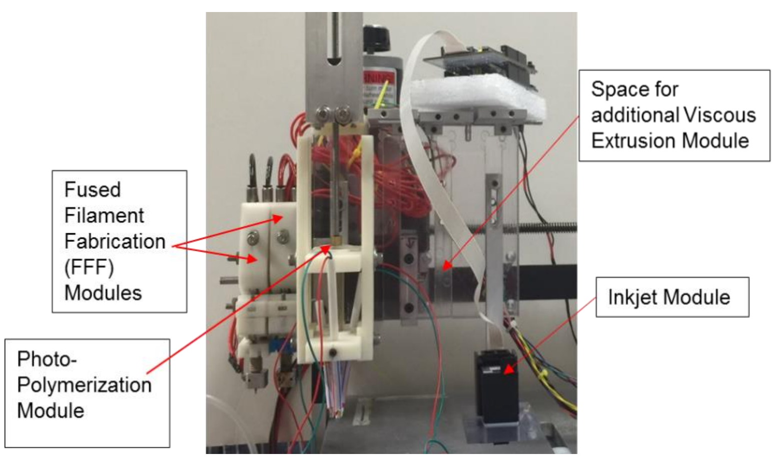

Figure 2.1 CMMB Setup [17]

2.1.1 Fused Filament Fabrication (FFF) Module

The multimodality BioPrinter at the MARS Lab is equipped with two FFF modules. The FFF module is also known as the Fused Deposition Modelling (FDM) (a term coined by Stratatsys). The FFF module consists of a marlin hot end and is interfaced by the RUMBA board through Marlin firmware. The FFF module has the capability to use materials with processing temperatures up to 260℃ such as ABS and PLA and supports 1.75mm diameter filament.

2.1.2 Photo-Polymerization (PP) Module

The Photo-Polymerization (PP) module of the CMMB is used to fabricate 3D objects using an UV adhesive resin which is in the form of gel. A variety of UV adhesive resin can used be for the purpose of constructing a 3D objects such as Solarez 3D printing resin, NEA123T [18], and UV15DC80 [19].

2.1.3 Inkjet Module [21]

The Inkjet (IJ) Module for the CMMB is used to dispense ink similar to a typical inkjet based 2D printer. The Inkjet module is based on HP hardware. The inkjet head is controlled using an Arduino Uno and a shield called Inkshield software.

2.2 Software

The software for 3D printing technology involve the design of CAD models in an appropriate modelling software and converting the model to Stereolithography (STL) format. The generated STL file is processed using a slicing or layering software which converts the STL file into G-code instructions based on the user defined process parameters which include layer height, wall thickness, print head speed, infill density, and support for the 3D printing client to execute.

2.2.1 *CAD Software and Stereolithography (STL)*

In this process, a 3D model is designed in an appropriate 3D modelling software such as Solidworks, CATIA, Pro-Engineer, and Rhino. A solid model for one of the PP LED holders is shown in Figure 2.2(a) designed in Solidworks 2015. The 3D model designed in CAD software is then converted to stereolithography format. STL is a file format which describes the triangulated representation of a 3D model without depicting model attributes such as color or other qualitative features. The triangulated representation of the solid model is shown in Figure 2.2(b).

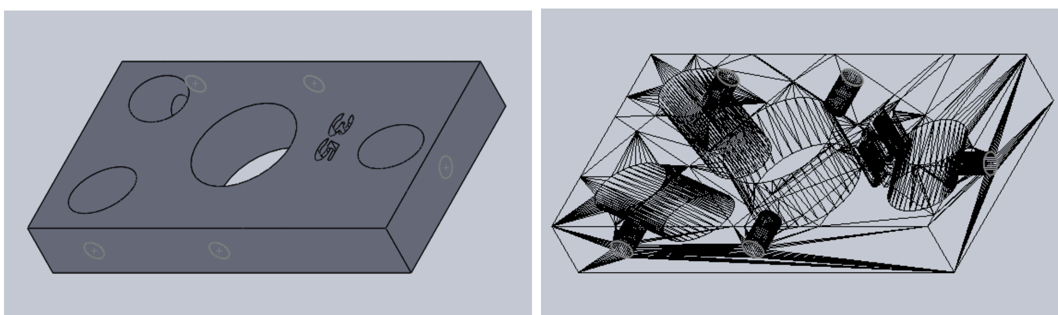

Figure 2.2 (a) CAD model for one of a LED fixture plates using Solidworks 2015,
(b) Triangular representation of solid model using the STL feature

2.2.2 *Slicer Software*

The function of slicer software is to convert a digital 3D model into a set of print instructions (usually in the form of G-code) depending upon the parameters defined by the user and the hardware specifications. There are various slicer software platforms available, both open and closed source. Open source slicer software includes Slic3r, Cura Engine, and Skeinforge. Closed software includes KISSlicer, and Simplify3D. The important parameters of a slicing software are layer height, fill density, fill pattern, print head speed for perimeters and infill structures, raft and support, filament diameter, extruder and bed temperature, and nozzle diameter.

The Slic3r graphical user interface for the definition of desired process parameters is shown in Figure 2.3.

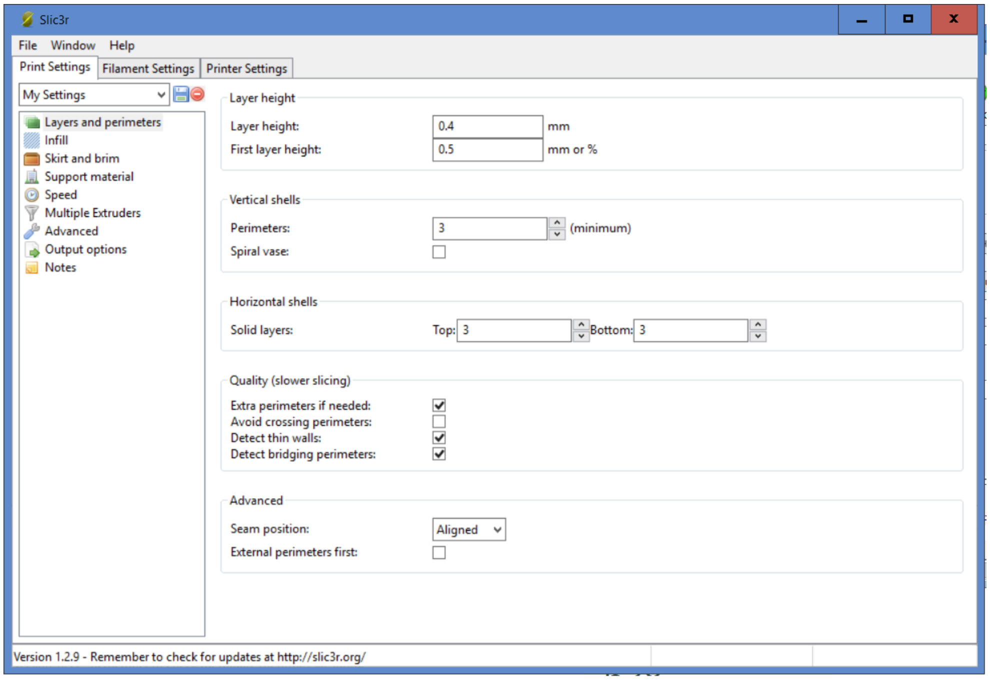

Figure 2.3 Slic3r GUI Software [20]

2.2.3 3D Printing Client

3D printing client is a software which is used to operate a 3D printer. There are various 3D printing clients available such as Repetier-Host, Pronterface, Matter Control, and Octoprint. In this work, the Repetier-Host 3D printing client was extensively used in the characterization experiments for the UV adhesive resin. Repetier-Host is a 3D printing client developed by Hot-World GmbH & Co. KG. Its function is to operate and control all the functions of the 3D printer to fabricate the required 3D object based on the G-code generated through a slicer software. The important features of Repetier-Host client include object placement, preview showing printing statistics such as length of filament needed, estimated print time, layer count and G-code editor. It also includes manual control for the 3D printer similar to a joystick. The printer settings such as communication port, baud rate, travel and Z-feed rate, manual extrusion and retraction speed, default extruder and bed temperature, build platform dimensions, firmware EEPROM information, units of objects which are imported and the preference settings are also included.

2.2.4 Marlin Firmware

Marlin firmware provides control, manipulation and data acquisition to the respective control board for operating a 3D printer. The Marlin firmware offers some important features such as PID control support for 3D printer, temperature oversampling, end stop switch interface, high step rate, interrupt based movement and interrupt based temperature protection [21].The Marlin firmware currently supports a number of 3D printer control boards including the RUMBA board used for the CMMB [21].

The RUMBA board is an electronic device which is used to control upto six stepper motors through Pololu pin compatible stepper drivers. It features an on-board ATmega2560.

In this chapter, the various modules associated with the multimodality BioPrinter were discussed. The slicer and 3D printing client software Slic3r and Repetier-Host were briefly introduced along with the Marlin firmware and RUMBA control board.

CHAPTER 3

PHOTO-POLYMERIZATION MODULE

3.1 Photo-Polymerization or Viscous Extrusion Module

The Photo-Polymerization (PP) module of the multimodality BioPrinter is a type of print head which is used to extrude liquid uncured polymer resin. This uncured resin is then solidified to a rigid structure through the application of an UV light source. In the PP process, a 3D object is fabricated by extruding one layer of uncured resin onto a build platform and then cross-linking the uncured layer using a UV light source. In the next step, another layer of uncured resin is laid on top of the previously cured resin and this new layer is cured. This process is repeated, layer by layer, until the desired final geometry is fabricated. Two designs were considered for the PP module setup and are discussed in Section 3.2.4.

3.2 Components for the Photo-Polymerization Module

The components of the PP module of the CMMB consists of a number of essential components which are introduced and discussed. One of the proposed designs for the PP module is shown in Figure 3.1.

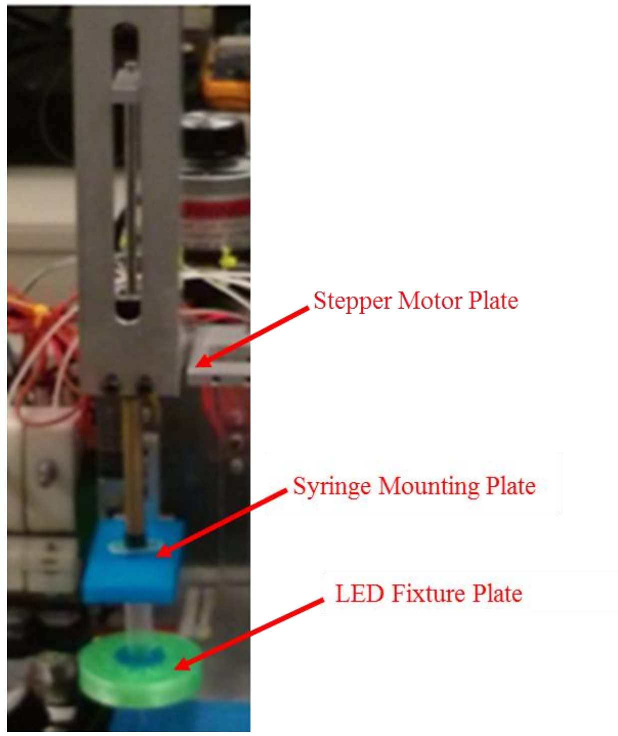

Figure 3.1 PP Module

The stepper motor plate is used to mount the stepper motor that acts as a linear actuator to push the 3D printing resin through the syringe nozzle based on the desired or defined feed (amount of resin displaced by the plunger).

A syringe mounting plate is used to mount a 3cc syringe containing the 3D photo-polymerizable printing resin. A slider is attached to the syringe mounting plate which is in turn is mounted onto the Plexiglas back-plate which is capable of housing three other modules. The UV LEDs considered in the current research are discussed in Section 3.4. Two designs of LED fixture plate were investigated and experimented with for the PP module setup.

a) An LED fixture plate with three LEDs at different angles of 20°, 25°, 30° and 35°. In this LED fixture plate, the LEDs are mounted at an appropriate angle. The purpose of this LED fixture plate is that the angle for the LEDs is adjusted such that the LED rays are directed at the extruding point. The following analysis was performed to identify the LED angle on the LED fixture plate. Figure 3.2 shows a schematic for evaluating inclination for mounting LEDs at an angle.

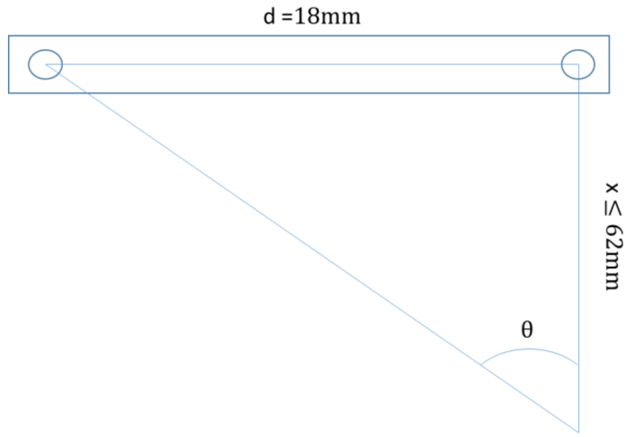

Figure 3.2 A Schematic for evaluating inclination angle for mounting LED at an angle

Inclination angle, θ for the LED is 15°, thus

$$\tan\theta = \frac{d}{x} \tag{3.1}$$

Where, d is the distance from the center of the syringe to the centre of the LED and is equal to 18mm. x is distance from the syringe tip to the LED fixture plate and depends upon the mounting angle of LEDs.

The distance from the syringe tip to the LED fixture plate for the angles considered of 20°, 25°, 30° and 35° is 50.00, 38.30. 31.00 and 25.70 mm respectively.

The length for the syringe considered is only 62mm and as such the angles 20°, 25°, 30°, and 35° can be considered as feasible option in the design of the LED fixture plate. The solid model of a LED fixture plate with 25° LED mounting angle is shown in Figure 3.3.

Figure 3.3 LED fixture plate with LEDs mounting angle of 25°

Figure 3.4 shows the PP module along with the LED fixture plate with LEDs mounted at angle of 25° with respect to the horizontal surface of the LED fixture plate.

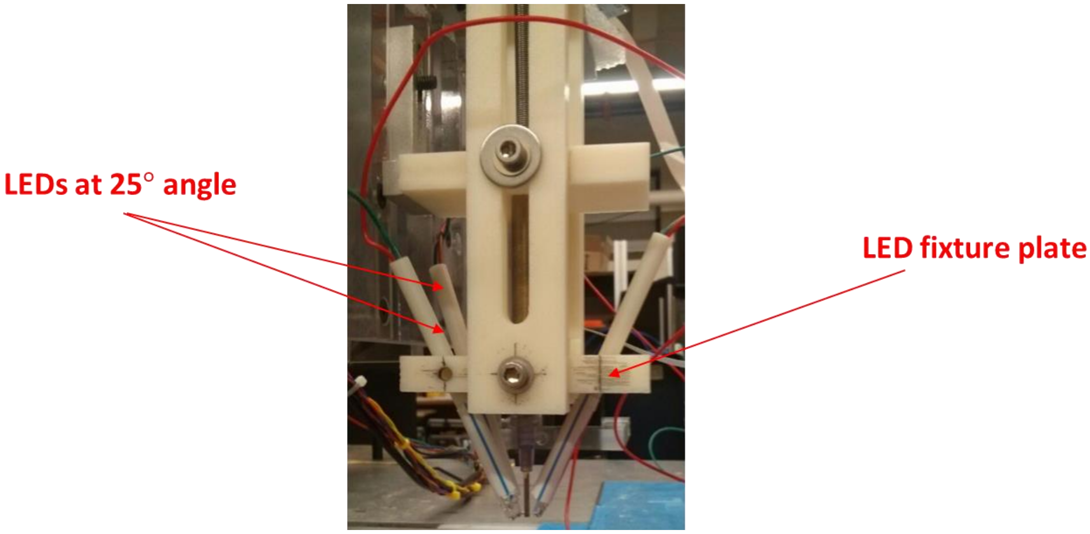

Figure 3.4 Photo-Polymerization module with LEDs mounted at 25° angle

(b) The LED fixture plate with circular LEDs arrangement.

The fixture plate shown in Figure 3.5 is used to mount LEDs perpendicular to the 3D printer bed with each LED at a distance of 6mm from the syringe tip and arranged in a circular fashion.

The purpose of having a circular arrangement is to cover the whole surface below the LEDs with UV light while fabricating any desired shape or while the head is moving in any direction.

Figure 3.5 LED fixture plate with circular arrangement of LEDs

This LED fixture plate is mounted at the bottom most portion of the workable syringe region and is capable of housing up to eight UV LEDs in a circular pattern. The purpose of having eight LEDs mounted on the fixture plate is to cover the entire region in a circular fashion on the build surface so that the resin would be able to polymerize while the print head moves in any given direction. Figure 3.6 shows a schematic of the region covered by the LED rays based on the circular LED fixture plate.

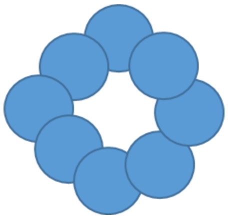

Figure 3.6 A schematic showing the region covered by UV LEDs

Figure 3.7 shows the PP module with the LED fixture plate based on circular arrangement of LEDs.

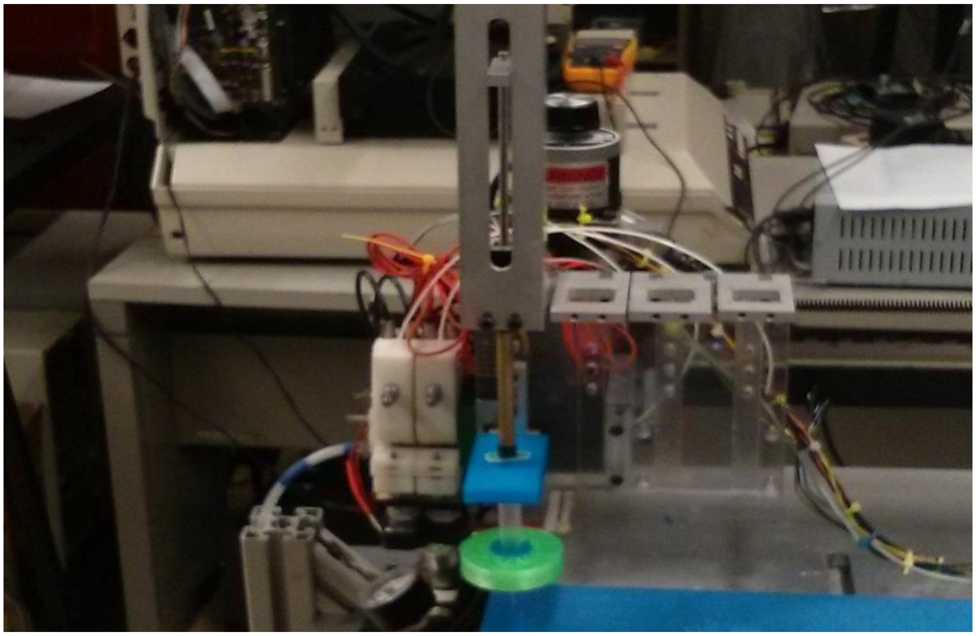

Figure 3.7 PP module with the LED fixture plate based on circular arrangement of LEDs

The only limitation with this LED fixture plate design is that due to the perpendicular mounting of the LEDs with respect to the printer bed, any object within the distance between the syringe tip and the centre of the LED (6mm in the case considered), for example a circle of 5 mm diameter, will not be able to polymerize and thus this area is considered as a Dead Zone (see Figure 3.8). The dead zone shown in figure 3.8 is applicable for LED mounted in a tube and is not applicable if the rays from the LEDs are diverging.

Figure 3.8 LED fixture plate with non-polymerizable area shown as Dead Zone

3.3 3D Printing Resin

A 3D printing resin consists of three major components, monomers, oligomers or binders and photo-initiators. When a layer of 3D printing resin is dispersed onto a build platform, the uncured layer of resin is usually cured within milliseconds to a few seconds depending upon the type of resin and intensity or power of the UV light. There are different UV curable 3D printing resin available such as Solarez [22], NEA123T [18], UV15DC80 [19], etc. Most of the resins available differ in viscosity, and curing time.

A typical 3D printing resin can be cured using three different methods, UV treatment, heat treatment and visible light treatment. The UV curing is usually the fastest and cures an uncured resin within milliseconds (such as Solarez resin) to a few seconds (such as NEA123T) depending upon the photo-initiator present in the polymer resin and also the power of the UV light as compared to heat treatment which can take from 10 min to a few hours for the uncured resin to polymerize depending upon the amount of heat supplied [18].

The 3D printer resin used to understand the PP process and its parameters and for the initial design and improvements on the module design is the Solarez 3D printing resin (http://solarez.com). A standard toothpaste is also used to compare viscosity effects via dimensional stability analysis with respect to the Solarez resin as discussed in Section 4.3.3.

A toothpaste which can be used to compare dimensional stability with Solarez resin is a time-dependent Non-Newtonian fluid in which the viscosity not only depends on the change in temperature but also on the shear rate. Toothpaste is considered to be a plastic fluid in which a certain shear stress has to be applied before flow can occur. The viscosity of standard toothpaste is 150,000-250,000 cps [23].

3.4 Ultraviolet (UV) Light Emitting Diodes (LEDs)

The main source required to activate the photo-initiator and thus initiate the process of PP reaction is the ultraviolet (UV) LEDs. The typical wavelength of an UV LED for PP reaction is between 320-405 nm. Most of the UV LEDs have their peak sensitivity at 365-390 nm for activation of photo-initiator.

3.4.1 Bivar Ultraviolet (UV) LEDs [24]

Bivar LEDs are tight tolerance LEDs having wavelength in the range of 390 nm to 405 nm and a tight tolerance of +/- 2.5 nm. The Bivar LEDs have a build-in Zener diode to protect the circuit from electrostatic discharge. The chip material for the Bivar LEDs is made from Indium Gallium Nitride/Sapphire and the emitting colour of the light is purple with a clear lens. The Bivar UV LEDs are available in two different viewing angle of 15° and 30°. The 30°viewing angle LEDs are used in the characterization experiments [24].

The UV LEDs used in the characterization experiments of the Solarez resin based on the various process parameter are Bivar UV LEDs with a wavelength of 390 nm and 3 mm diameter. The power of the Bivar LEDs can be adjusted by varying the supply voltage through an appropriate power supply.

3.4.2 Power Supply for the LEDs

The power supply is used to control the intensity of the UV light used to activate the photo-initiators present in the Solarez resin which initiates the PP process is from Pacific Photometric Instrumentation. The maximum output voltage available with this high voltage power supply is 2kV. The maximum output current possible is 10MA and depends on the voltage set by the user.

The Bivar UV LEDs are operated at a maximum voltage of 3.4V and minimum voltage of 3.0V. A circuit was developed to power the UV LEDs and the current was controlled by varying the operating voltage through the power supply.

3.5 Stepper Motor characteristics for syringe extrusion

The motor used for extruding the Solarez resin using the PP module is model 28F47-2.1-906 stepper motor linear actuator from Haydon Kerk [25].The stepper motor is a non-captive which means that the stepper motor has a lead screw going through the motor and has no stroke limit but the lead screw should be attached to non-rotating assembly for proper operation. A brass plunger is attached to the lead screw which in turn is used to controllably push the resin through the syringe nozzle.

This stepper motor shaft rotates1.8° per step. The amount of linear travel of lead screw attached to the stepper motor for one step is 0.00125 inch. The volume of resin displaced by the plunger is equal to the distance travelled by the plunger and depends upon the linear travel of the lead screw.

In the current chapter, the different components associated with the PP module were discussed. The two LED fixture plate designs were also discussed. The properties of the Solarez resin used in the characterization experiment were also introduced.

CHAPTER 4

CHARACTERIZATION EXPERIMENTS AND RESULTS

4.1 Process Parameters

There are various factors that affect the characterization of a 3D printing process. These factors can be classified as material dependent such as the viscosity of the 3D printing. They can be hardware dependent such as the print head speed (mm/min), nozzle to bed-distance (microns), nozzle diameter (microns), power of the UV LEDs (mW). It is also important to consider environmental dependent factors such as the temperature, and humidity.

The process parameters which are considered for the characterization of the Solarez 3D printing resin are directly controlled by the user are discussed in the following sub-sections.

4.1.1 Nozzle-to-Bed Distance

The nozzle-to-bed distance is the distance from the lowermost part of the syringe nozzle (needle) to the topmost surface of the build platform (bed). The larger the nozzle-to-bed distance, ideally more the height of the polymerized strand (up to microns' level). In this work, the nozzle-to-bed distance is measured in microns.

4.1.2 Nozzle Diameter

The nozzle diameter, which is the inner diameter (ID) of the syringe needle is directly proportional to width of the polymerized strand. The larger the ID of the nozzle, the larger the width of the polymerized strand. In this work, the nozzle diameter is measured in microns.

As an initial assumption, the cross section of the strand fabricated using the PP module can be approximated to a cuboid or a parallelepiped. The principle of volume conservation is used to calculate the feed which depends on the diameter of the nozzle used during the characterization of Solarez resin. The nozzles used were during the characterization experiments were 417µm, 468 µm and 566µm diameter.

In this feed calculation, the volume of the fluid (3D printing resin) being pushed by the syringe plunger is equal to the volume of fluid (Solarez resin) exiting the syringe nozzle, according to the principle of volume conservation. Figure 4.1 shows a schematic of a Syringe extrusion process with the necessary parameters.

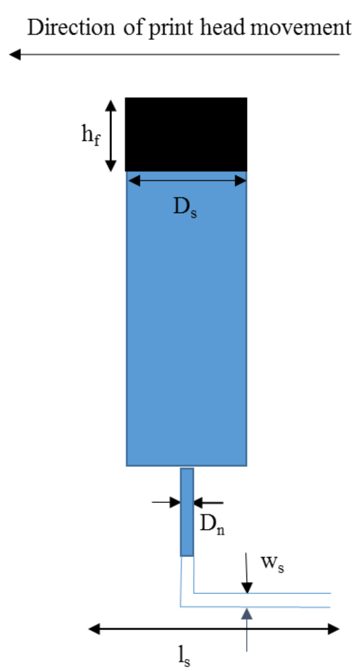

Figure 4.1 Schematic of Syringe Extrusion Process

Volume of resin pushed out by the syringe plunger can be presented in the following equation

$$V_s = \frac{(\mathrm{\pi D_s^2})}{4} * \mathrm{h_f} \tag{4.1}$$

Where, $\mathrm{D_s}$ is the Internal Diameter (I.D.) of the Syringe (µm) and $\mathrm{h_f}$ is the feed (distance travelled by the plunger)

The volume of the fluid (Solarez resin) exiting the syringe nozzle can be presented in the following equation

$$V_f = \frac{(\mathrm{\pi D_s^2})}{4} * \mathrm{h_f} \tag{4.2}$$

Where, $\mathrm{D_n}$ is ID of the Syringe nozzle (µm) and $\mathrm{l_s}$ is the length of the strand fabricated (mm)

Setting equations (4.1) and (4.2) equal, it can be concluded that, the amount of resin displaced by the plunger is given by Equation (4.4).

$$\mathrm{h_f} = \left(\frac{D_n}{D_s}\right)^2 \mathrm{l_s} \tag{4.3}$$

Also, the volume of the fluid being pushed out by the plunger or the volume of the fluid exiting the nozzle should be equal to volume of the strand being fabricated to preserve the volume conservation principle of volume conservation.

i.e. $$\frac{(\mathrm{\pi D_s^2})}{4} * \mathrm{h_f} = \frac{\mathrm{\pi D_n^2}}{4} * \mathrm{l_s} = \mathrm{l_s} * \mathrm{w_s} * \mathrm{h_s} \tag{4.4}$$

Where, $\mathrm{w_s}$ is the width of the strand (microns), considering the cross section to have cuboid profile and $\mathrm{h_s}$ is the height or thickness of the strand (microns)

But it should be noted that, the viscosity of the resin used for the characterization experiment plays an important role in affecting the geometry of the strand and could result in violating Equation (4.5) due to the low viscosity of the resin. The calculation for feed values for nozzle diameter 417µm, 468µm, ad 566 µm based on Equation (4.3) are provided in Appendix A and final results are provided in Table 4.1.

Table 4.1 Feed value based on different nozzle diameter

Nozzle Diameter (µm)	Feed Value (µm)
417	260
468	320
566	470

4.1.3 Print Head Speed

The print head speed (mm/min) is the speed at which the 3D printer extruder is operated. The print head speed and the feed, which is the amount of material pushed out by the plunger from the syringe nozzle are coordinated. The feed values for the nozzles considered during the characterization experiment can be calculated using the volume conservation principle as discussed in previous section. Also, the plunger and the print head have a coordinated motion.

4.1.4 Intensity or Power of the LEDs

The solidification or hardening of the polymerized strand depend on the intensity or the power of the UV LED. The power of the LED can be calculated by measuring the applied voltage and forward current. The maximum forward voltage at which the Bivar UV LED (considered in the current work) can be operated is 3.4 V and this corresponds to 20mA forward current according to the manufacture [24]. The power of the LED corresponding to value of voltage and current mentioned is found to be 68mW ($P = VI = 3.4\,V \times 20\,mA = 68\,mW$). The intensity of the LED rays directed on a given platform is directly proportional to the power of LED and inversely proportional to the distance of the LED from the platform (where the LED rays are directed). The intensity is also proportional to the rate of polymerization of resin, i.e. more the intensity of the UV light, higher the polymerization rate of the resin. Hence, the combination of the power of the LED and its distance from the platform affects the polymerization of the strand.

The process parameter values for the characterization experiments and Design of Experiments (Design-Expert®, Minneapolis, MN, USA), analysis are performed based on some initial experiments conducted.

4.2 Characterization Experiments using different LED fixture plates

The characterization experiments of the Solarez resin are performed using the two LED fixture plate discussed in Section 3.2.

4.2.1 Characterization Experiment using LED fixture with LEDs mounted at an appropriate angle

The purpose of this LED fixture plate design is to direct the LED at the extrusion point by mounting the LEDs at an appropriate angle with respect to the horizontal surface of the LED fixture plate. In this work, the LED fixture plate with three LEDs at an angle of 20°, 25°,30° and 35° with respect to the horizontal surface of the LED plate is used.

The process parameters considered in the characterization experiments of the Solarez resin and as mentioned in Section 4.1 are: nozzle-to-bed distance, print head speed, feed (or nozzle diameter) and power of the LED. The UV rays in this fixture plate are directed below the extruding location after adjusting the fixture plate with respect to the syringe lowermost workable region according to nozzle tip and due to the exceptionally fast curing nature of a 3D printing resin, the

UV rays end up clogging the tip of the syringe nozzle thus preventing extrusion. Figure 4.2 shows a sketch showing the clogging of the nozzle.

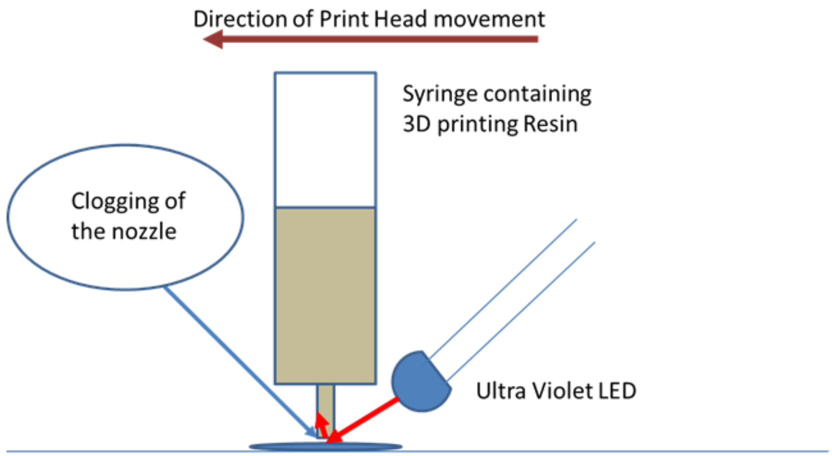

Figure 4.2 Representation of UV light directed below the extruding location

An improved design would be to mount LEDs perpendicular to the 3D printer bed while maintaining a sufficient distance between the LED and the syringe tip to avoid clogging. The sketch in Figure 4.3 shows an improved design that can be adopted for constructing LED fixture plate.

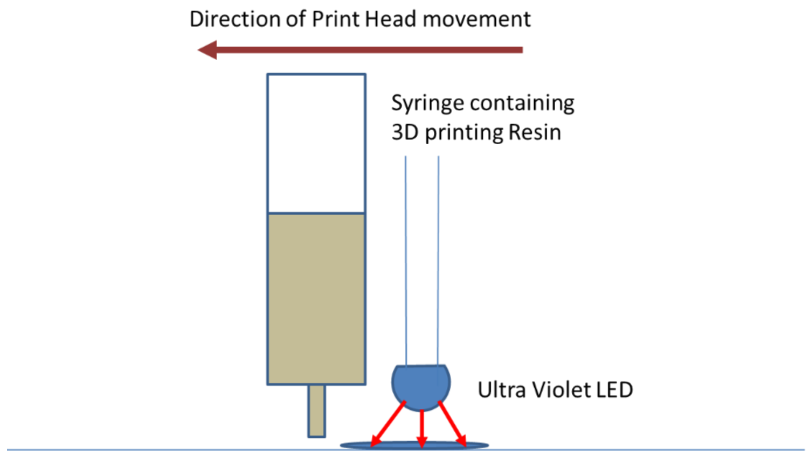

Figure 4.3 Improved model representing UV light fired vertically down avoiding clogging of the nozzle

The improved design of the LED fixture plate with a safe distance between the LED and the syringe to prevent clogging of the syringe nozzle is discussed in Section 4.2.2.

The characterization experiment of the resin was performed using LED fixture plate with LEDs at the 35° angle. Table 4.2 provides the parameters values considered in the characterization experiment.

Table 4.2 Process parameters for the characterization of resin using LED fixture plate at 35°

Parameters	Values
Nozzle-to-bed distance	200µm
Nozzle diameter	417µm
Power of LED	68mW
Print head speed	100mm/min

Figure 4.4 shows the characterization of the Solarez resin using the 35° LED angle plate.

Figure 4.4 Clogging of the nozzle with LED mounted at angle of 35°

From Figure 4.4, it is observed that although the UV rays falling at the point of extrusion instantly polymerizes the resin, the nozzle to bed distance is 200µm, and with LEDs mounted at an angle, some rays of UV light fall on the syringe tip. This causes the clogging of the nozzle due to the polymerization of the Solarez resin which takes place within milliseconds as specified by the manufacturer.

The DOE analysis using this design method might not be feasible due to improper extrusion/clogging of the syringe nozzle. To prevent the clogging of the syringe nozzle, the alternate design method with circular LED arrangement is suggested and is discussed in following section.

4.2.2 Characterization Experiment using LED plate with circular LED arrangements

The LED fixture plate with circular LED arrangement (refer to Figure 3.5) was used for this characterization work. This fixture plate has the advantage that there is an offset between the LED and the nozzle tip which prevents the clogging of the nozzle. One the other hand, polymerization of the resin is delayed, which leads to sagging of the resin. The offset distance between the centre of nozzle tip and the centre of LED is 6mm. This offset distance is the minimum distance possible between the centre of LED and nozzle tip such that the polymerization of extruded resin takes place without clogging of the nozzle. Hence, the time the LED takes to reach the extruded resin (t_l) is given by Equation 4.5.

$$t_l = \frac{d}{v} \tag{4.5}$$

Where, d is the offset distance between the centre of LED and nozzle tip (mm) and v is the print head speed (mm/min)

Table 4.3 provides the values for the process parameters considered in the characterization experiments.

Table 4.3 Process parameter values for DOE analysis

Process Parameters	Values
Nozzle-to-bed distance	100, 150 and 200 µm
Print head speed	100, 150 and 200 mm/min
Nozzle diameter (feed value)	417, 468, and 566 µm (0.26, 0.32, 0.47 mm)
Power of the LED	32, 49.5, and 68 mW

4.2.3 Design of Experiment analysis using Design-Expert Software

The characterization experiments of the Solarez resin are analysed in the Design of Experiment software, Design-Expert from Stat Ease using the LED fixture plate with circular arrangement. The design method that was considered in the characterization process is Optimality I-method. The Optimality I-method is used since the primary goal of the characterization experiment is to draw inference from the response data. The response data corresponds to the width and the thickness of the polymerized strand.

Appendix C provides the DOE runs generated for the process parameters based on the Optimality I-design method. The characterization experiments were then preformed based on the runs generated by the DOE software in the order it was generated. Figure 4.5 shows the strands fabricated based on the runs generated using the design expert software.

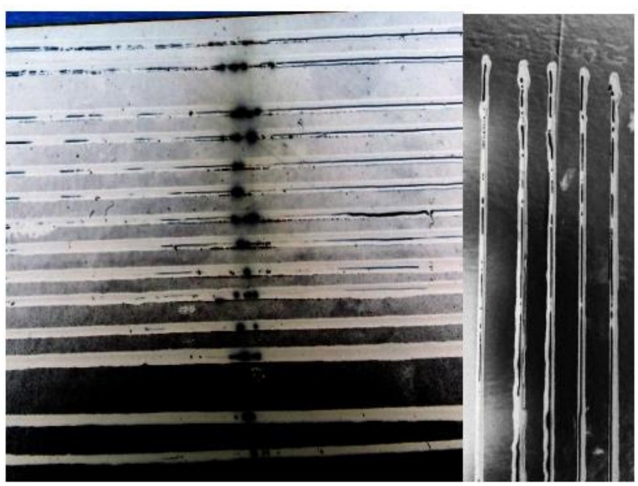

Figure 4.5 Strand fabricated based on the runs generated using Design-Expert Software

The characterization experiment is also affected by the viscosity of the resin apart from the process parameters defined in Section 4.1. For a successful characterization experiment for DOE analysis, a stable strand should be generated. The Solarez resin used in the characterization experiment has a low viscosity value (600 cps) and does not produce a stable strand, and thus affects the characterization of the resin which provides the response data (i.e. width and height of the strand) generated for the DOE analysis. Figure 4.6 shows the microscope pictures of three strands fabricated using the 417µm nozzle, nozzle-to-bed distance of 200µm, LED power of 68mW, and print speed of 100, 150 and 200mm/min from the DOE generated runs.

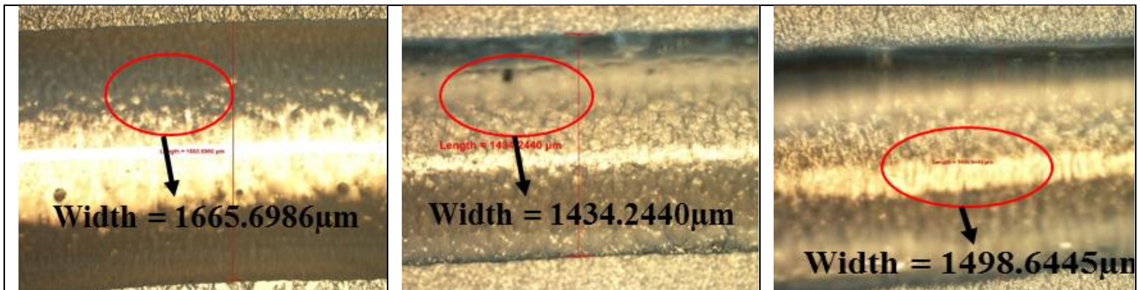

Strand 1	Strand 2	Strand 3
Width of the strand = 1665.70µm	Width of the strand = 1434.24µm	Width of the strand = 1498.64µm
Print speed = 100mm/min	Print speed = 150mm/min	Print speed = 200mm/min

Figure 4.6 Microscope Images of the strands fabricated using nozzle diameter of 417 µm and other process parameters

For a stable strand, the width and the height of the strand is expected to be close to the nozzle diameter and nozzle-to-bed distance respectively with a few degrees of error. The geometry (width and height) of the strand should be controlled so that each strand (layer) achieves the desired accuracy and precision responsible for building a 3D object.

For a successful DOE analysis, the characterization experiment should generate a dimensionally stable strand. Thus, it is suggested that the viscosity of the Solarez resin should be increased without significant impact on the polymerization characteristics before a full DOE analysis can be performed.

4.3 Effect of viscosity on the strands generated

In this section, the effect of viscosity on the strands fabricated using the PP module is analysed by quantitatively evaluating the expected width of the strand using the principle of volume conservation and comparing the dimensional stability of the Solarez resin with respect to a standard toothpaste. The purpose of using a toothpaste, which has viscosity in the range of 150,000-250,000 centipoise, proves to be a good material to be tested against a low viscosity resin such as the Solarez resin for dimensional stability analysis.

4.3.1 Evaluation of expected (theoretical) width of the strand and its relationship with the viscosity of the 3D printing resin

The principle of volume conservation is used to calculate the width of the strand. The volume of the resin displaced by the plunger is equal to the volume of the resin exiting the nozzle for volume conservation to be preserved. In other words, mathematically this can be represented using the following equality,

$$\pi \frac{{D_s}^2}{4} h_f = \pi \frac{{w_s}^2}{4} l_s \tag{4.6}$$

$$ {D_s}^2 h_f = {w_s}^2 l_s \tag{4.7}$$

Where, D_s is the internal diameter of the syringe (mm), h_f is feed (amount of plunger movement) (microns), w_s is the expected width of the strand (microns) and l_s is the length of the strand (mm).

From Equation (4.7), it should be noted that the internal diameter of the syringe (D_s) and width (w_s) of the strand for a particular run are assumed to be constant and are not dependent on time t, although there will be minor variation in the width of the strand due to the surface roughness of the print bed.

The width of the strand generated from Equation (4.7) is provided in Equation (4.8)

$$w_s = D_s\sqrt{\frac{h_f}{l_s}} \tag{4.8}$$

The plunger speed is not available directly but can be obtained from the distance travelled by plunger and the time taken by the plunger to move that particular distance. The calculation for the width of the strand in terms of the plunger speed (v_p) and print head speed (v_H) is provided in Appendix A. The width of the strand is expected to be close to the diameter of the nozzle considered, for dimensionally stability.

4.3.2 Characterization experiments for the variation in the width of the strand as function of viscosity

Three strands of Solarez resin were fabricated using the 417µm diameter nozzle. The power of the LED and the nozzle-to-bed distance were set to be 68mW and 200µm respectively. The print head speed was set at 100, 150 and 200 mm/min for the three strands. The purpose of the experiment was to verify whether the theoretical (or expected) value for the width of the strand is equal to the observed width of the strand.

After the strands were fabricated, it was observed from the Nikon microscope (refer to Figure 4.7) that the width of the strands is 3-4 times the expected value due to the low viscosity of the Solarez resin. This low viscosity is responsible for the poor dimensional stability of Solarez resin due to which the resin sag as it is laid on the build platform.

4.3.3 Dimensional Stability Analysis: Solarez vs Toothpaste

The Solarez 3D printing resin tends to sag due to its low viscosity. A characterization experiment was conducted using a standard toothpaste. The strand generated using the toothpaste was found to be more responsive to equation (4.7) because the toothpaste is about 75-125 times more viscous than the Solarez 3D printing resin. The viscosity of Solarez 3D printer resin as specified by the user is 600 cps whereas the viscosity of a standard toothpaste is in the range of 150,000-250,000 cps [23]. Table 4.4 provides the process parameters that were considered in the characterization experiment for the dimensional stability between the Solarez resin and a toothpaste.

Table 4.4 Process Parameter setting for dimensional stability analysis using Solarez resin and toothpaste

Process Parameters	Value
Print Head Speed	100mm/min
Nozzle Diameter	417µm
Feed (Amount of resin displaced by the plunger)	0.26mm

Table 4.4 Continued

Power of LED (only for Solarez resin)	68mW
Nozzle-to-Bed Distance	200µm
Length of the Strand Fabricated	100mm

The Solarez resin and toothpaste strand were fabricated using the PP module based on the process parameters defined in Table 4.4. The strand fabricated for the Solarez resin and toothpaste are shown in Figure 4.7.

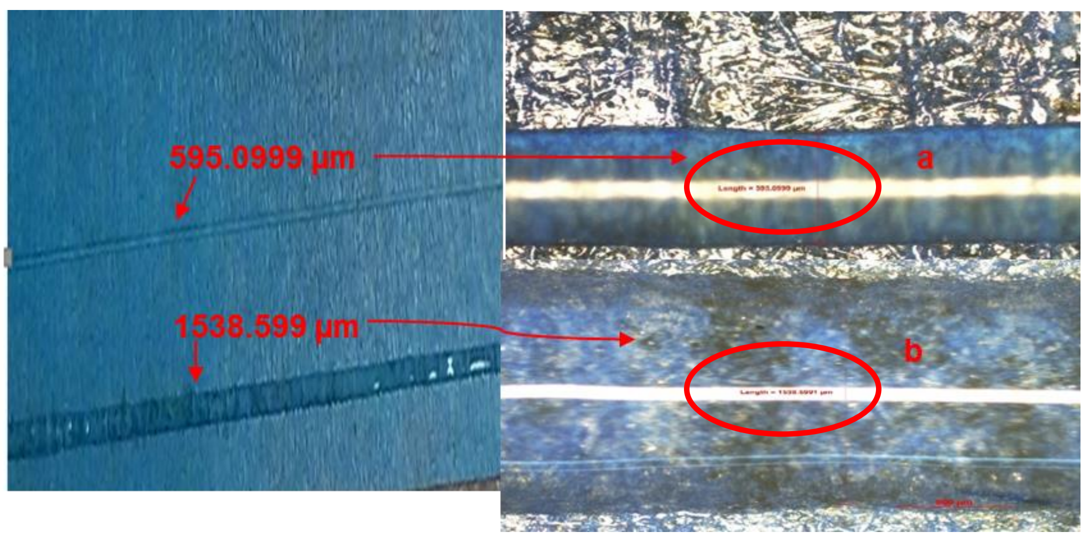

Figure 4.7 Representative strand fabricated using (a) Toothpaste, and

(b) Solarez 3D printing resin

The strand fabricated using the Solarez resin and the toothpaste were observed under the Nikon microscope. From the observation made, it can be concluded that due to the low viscosity of the Solarez resin, it sags after being extruded on the build platform and hence the width of the strand is about 3-4 times the nozzle diameter. On the other hand, the width of the strand fabricated using a standard toothpaste (viscosity = 150,000 cps) is much closer to the nozzle diameter. This is due to the fact that the toothpaste because of its high viscosity does not sag after extrusion.

4.4 Methods to improve dimensional stability of the Solarez resin

There are two methods that can be adopted to increase the viscosity of the resin so that the effects of viscosity can be reduced on the width of the strand fabricated. In the first method, the Solarez resin can be frozen to a temperature for the resin produce a stable filament, since the viscosity of fluid is inversely proportional to its temperature.

The second method involves doping of the resin. 3D printing resins such as NEA123T [18], UV150DC [19] can be doped with appropriate amount of nano-particles or nano-fillers to increase their viscosity in order to have better dimensional stability. The primary rational for using high viscosity resins such as ones mentioned is that the viscosity of the resin should be moderate to high for stable filament extrusion. The NEA123T resin has a viscosity of 200,000-300,000 cps whereas the viscosity of UV150DC is 40,000-50,000 cps. The Solarez resin has a viscosity of 600 cps and requires additional processing to increase the viscosity by temperature reduction or polymer doping.

Researchers from Ecole Polytechnique de Montreal developed UV assisted 3D printing (3DP) to manufacture photopolymers based on micro devices with 3D self-supported and freeform structures [26]. The resins that were used in the experiments were NEA123MB [27] and NEA123T [18]. In the experiments conducted, the NEA123MB resin was doped with 5 weight percentage silica nano-particles. This caused the viscosity to go up by 17 fold at low shear and also a shear thinning rheological behaviour. The other resin NEA123T was already doped with nanoparticles by the manufacturer and was used as received. Also, the NEA123T resin was doped with 0.5 weight percentage Carbon Nanotubes (CNTs). The viscosity increased with an increase in concentration to 1 and 2 weight percentage. The pure form of NEA123MB was used to fabricate a micro spring. But, it was observed that due to its low viscosity, it did not generate a stable strand. The doped NEA123MB and the NEA123T were then tested and it lead to the successful fabrication of a stable strand. Thus, it was concluded from the experimentation, that higher viscosity leads to a more stable strand.

The method of doping and freezing the resin have their advantages and disadvantages. The doping of a low viscosity resin using nano-particles or nano-fillers is a costly affair whereas maintaining the resin to a temperature suitable to generate a stable strand is difficult. The other limitation of freezing the resin is that the polymerization rate could be affected by lowering the temperature of the resin whereas, the concentration of doping the polymer resin should be such that it does not suppress the ability of photo-initiators present in the polymer resin. On the other hand, there is no temperature control required for doping a low viscosity resin and freezing the resin is an inexpensive process.

The methods considered in the current research for freezing the resin to a temperature sufficient enough to generate a stable filament are discussed in the following subsections.

4.4.1 Peltier thermoelectric cooling system

A Peltier thermoelectric cooling device uses the Peltier effect to create heat flux between the junctions of two different materials [28] . When a Peltier thermoelectric cooler is used as a cooling device, voltage is supplied across the device which leads to a temperature difference between the two sides of the thermoelectric device [29]. A heat sink is then used on the hot end side of the cooler to dissipate the heat and a fan can also be attached to the heat sink so as to draw more amount of heat from the cold end. The hot side of the thermoelectric cooler takes away the heat generated so that the other side becomes cooler. The function of the heat sink with a fan attached is to keep the hot end at ambient temperature.

The Solarez 3D printing resin viscosity can be increased by cooling the PP module assembly using thermoelectric coolers. Figure 4.8 show a sketch of the PP assembly showing Aluminium jacket and Peltier thermoelectric cooling system (not shown in the sketch) attached on the exterior of the aluminium jacket.

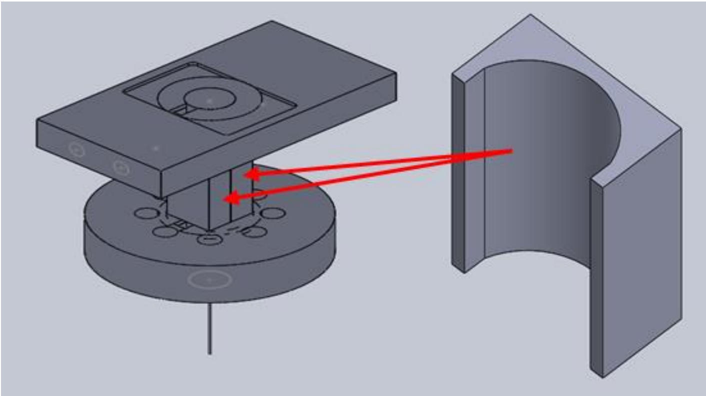

Figure 4.8 Peltier thermoelectric cooling system assembly consisting of aluminium jacket

The limitation of Peltier thermoelectric cooler is its low efficiency. For a 40mm x 40mm thermoelectric cooler, the heat sink and fan required is about 90mm x 90mm and it is not possible to incorporate such a bulky design due to the restricted space available on the PP module.

4.4.2 Double wall insulated jacket made from Acrylonitrile Butadiene Styrene (ABS)

Acrylonitrile Butadiene Styrene (ABS) is a type of plastic commonly used as a raw material for Fused Filament Fabrication (FFF) 3D printing applications. Since ABS plastic acts as an insulator, it can be used for the application of keeping the resin at a cold temperature for a longer period of time after it has been stored in a freezer for a certain period. For this purpose, a double wall insulated jacket with an air gap between the walls as shown in figure 4.9, was developed using ABS plastic on a FFF based 3D printer. The purpose of having an air gap between the walls was to take advantage of the thermal conductivity of air which is 0.024 W/mK. The thermal conductivity of the ABS plastic is in the range of 0.14-0.21 W/mK and thus air acts as a third insulation medium, the other two being the walls of ABS, and impede the rapid rise of temperature of the resin. Figure 4.9 shows the double wall insulated jacket prototyped using ABS 3D printing material.

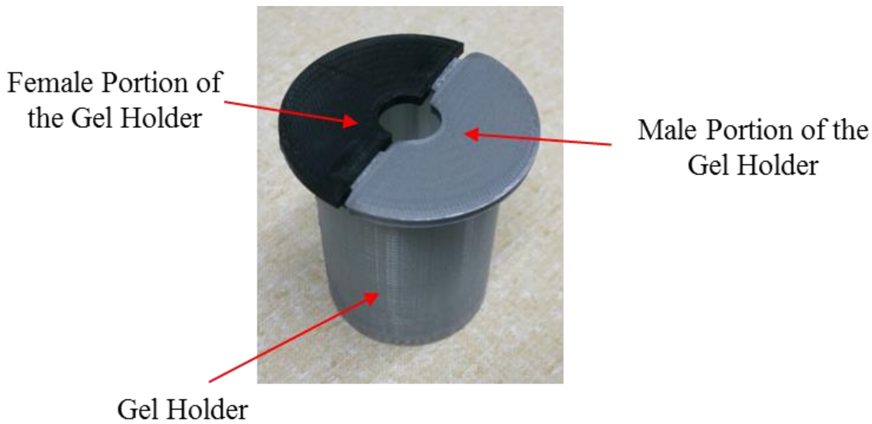

Figure 4.9 Coolant gel holder

4.4.3 Qualitative analysis for the change in the Viscosity of Solarez resin as a function of temperature and time elapsed

In this work, the Solarez resin at (26°C) was frozen in a conventional freezer for 24 hours. The ambient temperature was 26°C. The initial temperature of the frozen resin was measured by interfacing LabVIEW [30] with the same thermocouple used for measuring the ambient temperature. The temperature of the resin was found to be -20°C.

The input comes from the voltage supplied by the thermocouple and the sampling rate corresponds to the sample supplied by the user. One sample corresponds to 10 seconds. LabVIEW measures voltage coming from the thermocouple and this voltage obtained from the thermocouple is converted to temperature using a calibration curve. The calibration equation is given by Equation (4.7).

$$\text{Temperature (°C)} = 25 + \left(\frac{60-24}{5.10199-2.0285}\right)(\text{Voltage} + 5.10199) \tag{4.7}$$

The output is the data generated for the temperature of the resin as a function of time (refer to Appendix C) and is shown in the form of waveform and the time and temperature data collected is stored as in a spread sheet. Figure 4.10 shows the graphical representation of the data generated using the LabVIEW interfaced thermocouple for measuring the temperature of the Solarez resin as a function of time elapsed.

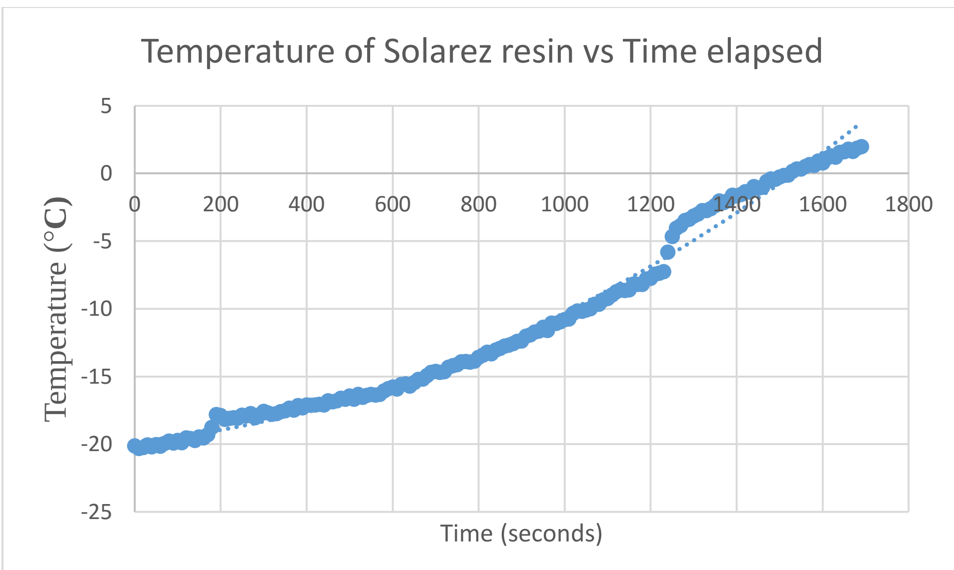

Figure 4.10 Graphical representation of temperature measurement of the Solarez resin as a function of time using LabVIEW

Figure 4.10 can be used to analyse the critical time for the Solarez resin to remain stable for the characterization experiment. For example, if the critical temperature of the resin is found out to be 0°C, then the user would have about 25 minutes to perform the characterization experiment before the Solarez resin losses its stability.

4.5 Study of the cross-section of the strand fabricated using Solarez 3D printing resin

A series of characterization experiments were conducted to study the cross-sectional behaviour of the strand constructed using Solarez 3D printing resin. The temperature of the resin was at 26°C. Table 4.5 provides the process parameter values considered for the analysis of the cross-section of the strand.

Table 4.5 Process Parameters for study of the cross-section of a strand fabricated using PP using Solarez resin

Parameters	Value
Feed Rate (Velocity of the Print Head)	100, 150 and 200 mm/min
Nozzle Diameter	$417\mu m$
Feed (Amount of resin displaced by the plunger)	0.26mm
Power of LED	68mW
Nozzle-to-bed distance	$200\mu m$
Length of the Strand fabricated	100mm

Figure 4.11 provides the images taken from the Nikon microscope for the strand fabricated using the Solarez resin based on different print head speeds. The geometry of the strand is observed to be a segment of the circle in each of the three cases considered.

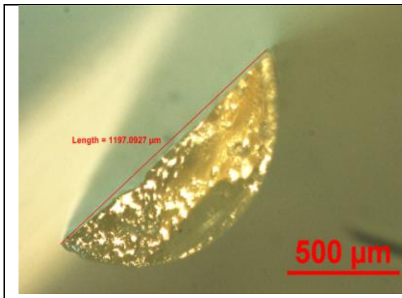	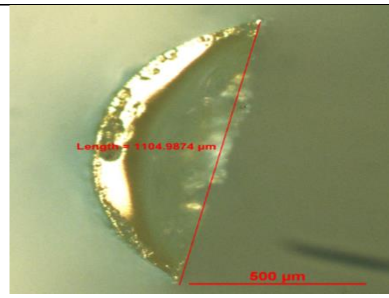	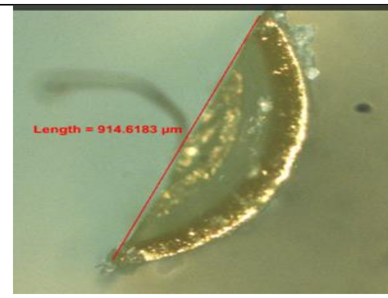
Cross-section of strand for Print Speed of 100mm/min Scale Bar 500 microns	Cross-section of strand for Print Speed of 150mm/min Scale Bar 500 microns	Cross-section of strand for Print Speed of 150mm/min Scale Bar 500 microns

Figure 4.11 Cross section of Solarez polymerized strand with different print head speeds

4.5.1 Quantitative analysis of Photo-Polymerized strand cross section

In Section 4.1, the feed value (amount of resin displaced by the plunger) was calculated based on the principle of volume conservation by equating the volume displaced by the plunger to the volume of resin exiting the nozzle. The profile of the strand fabricated was not taken into account.

In this section, the feed value will be calculated for the strand which is observed to have segment of a circle profile and will be compared with the feed value calculated using the initial assumption (strand with parallelepiped profile). In this work, it is assumed that there is no compressibility (no air gap between the plunger and the resin when the plunger is displaced to extrude the resin) and the effects of the viscosity of the resin are neglected.

Figure 4.12 shows the observed segment of a circle profile for the strands fabricated.

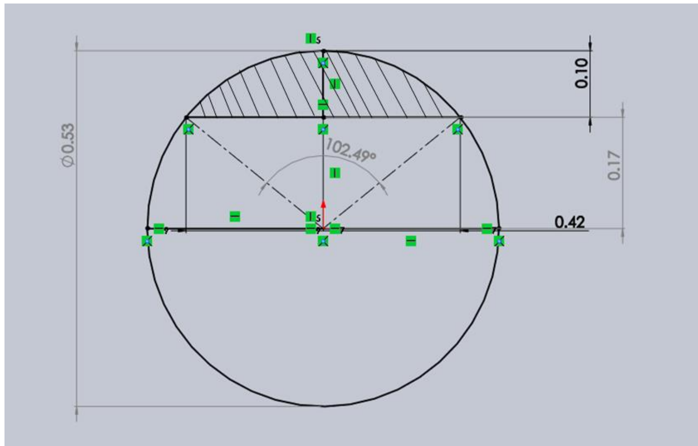

Figure 4.12 Photo-Polymerized strand having a segment of a circle profile

In the analysis, the volume conservation principle is used to equate the volume of the resin exiting the nozzle to the volume of the strand fabricated. The calculation for the volume of the strand and the feed value required for the 417µm nozzle for the initially assumed profile (parallelepiped profile) and the observed profile (segment of circle) are discussed in Appendix A and the results are given in Table 4.6.

Table 4.6 Volume and feed value for the strand using 417µm nozzle diameter

Strand Profile	Volume(mm^3)	Feed Value (µm)
Parallelepiped	4.17	78.00
Segment of circle	2.50	47.00

The feed values calculated using the volume conservation principle while equating the volume of resin displaced by plunger equal to volume of the resin exiting the nozzle for nozzle diameter of 417µm was found out to be 260µm. This is due to the reason that; it was assumed that resin exiting the nozzle had a cylindrical profile (refer to Section 4.1.2). On the other hand, the feed values calculated and shown in Table 4.6 for 417µm nozzle are 78µm and 47µm. This is because these feed values are calculated based on conserving the volume by equating volume displaced by the plunger to volume of strand fabricated and the profile for the strand which were laid on the build platform were considered to have parallelepiped profile (initially assumed profile for strand) and segment of circle profile (observed profile) respectively.

This chapter discussed the process parameters considered in the characterization of the Solarez resin. It discusses the characterization experiments performed using the two LED fixture plate design discussed in Chapter 3. The results obtained from the characterization experiments are also discussed. It also evaluates the effect of viscosity on the characterization experiments.

CHAPTER 5

CONCLUSION AND FUTURE WORK

The rapid development of additive manufacturing and 3D printing technologies have increased the demand for producing prototypes in any given field, be it arts, engineering, food industry, sports due to its cost effectiveness. The additive manufacturing (AM) technology can ensure precession, accuracy, strength and high quality products. The multimodality BioPrinter setup developed by Manufacturing Automation and Robotics System (MARS) Lab at University of Texas at Arlington is used to develop and investigate the capabilities of various 3D printing technologies such as Fused Filament Fabrication (FFF), Photo-Polymerization (PP) or Viscous Extrusion (VE), and Inkjet (IJ) printing on a single 3D printer. In this research, PP or VE module was developed and process parameters affecting the characterization of 3D printing resin were identified. The effects of viscosity on the characterization of the resin and the cross sectional behaviour of the strands fabricated using PP module were also investigated.

5.1 Conclusion

The Photo-Polymerization (PP) module for the multimodality BioPrinter is developed and the various process parameters affecting the characterization of the Solarez resin are identified. The effect of viscosity on the characterization of the Solarez resin are studied experimentally in terms of dimensional stability. The important accomplishments of this research work are:

- Characterization experiments are performed to study the effects of viscosity on less viscous 3D printing resin.
- Dimensional stability analysis between a standard toothpaste (viscosity = 200,000 cps) and Solarez resin (viscosity = 600cps) showing the Solarez resin inability to maintain structural

rigidity. It tends to sag when dispensed onto the build platform in comparison with the toothpaste which has much better stability due to its high viscosity.

- Investigated the cross section of the strand comparing a circle profile rather than the parallelepiped profile originally considered.

5.2 Future Work

The negative effects of viscosity in terms of stability on the characterization of the low viscous Solarez resin need to be addressed in order to take advantage of the developed PP module. Also, an effective method to increase the viscosity of the Solarez resin needs to be identified to minimize the effects of viscosity and hence improve the dimensional stability of the resin. To enhance the capabilities of the current PP module setup, suggestion for the future work include:

- Investigation of the characterization of a high viscous resin such as NEA123T [18](viscosity = 300,000-400,000 cps) where the effects of viscosity are minimal.
- Find an effective method of improving (increasing) the viscosity of low viscous resin using doping with nanoparticles or nanofillers [26].
- Develop a controlled environment for the PP setup.
- Perform a Design of Experiment analysis on the improved or high viscous resin (where the effects of viscosity are minimal) using any of the Design of Experiment package available.
- Study the relationship between the various process parameters using the Design of Experiment analysis.

This chapter provided an overview about the characterization of the Solarez resin and suggested methods that can be adopted for successful characterization of any polymer resin.

APPENDIX A

DERIVATION OF EQUATIONS AND MATHEMATICAL CALCULATIONS

A.1 Calculation of the feed (amount of 3D printing resin displaced by the plunger)

Figure A.1 shows a schematic representation of the syringe extrusion with the parameters affecting the feed (amount of resin displaced by the plunger)

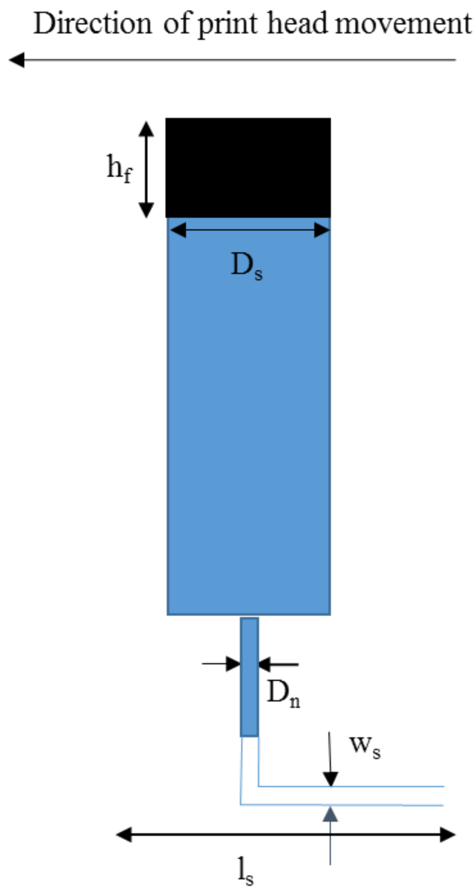

Figure A.1 Schematic of Syringe Extrusion Process

The following is the calculation of feed for nozzle diameter using the following parameters. D_n = 417µm, l_s = 100mm, D_s = 8.25mm

Volume of fluid (3D printing resin) being pushed out by the syringe plunger can be modelled in the following way,

$$V_f = \frac{(\pi D_s^2)}{4} * h_f$$

$$= \frac{(\pi * 8.25^2)}{4} * h_f$$

Hence,

$$V_f = \frac{68.0625}{4} \pi h_f \qquad \text{(A.1)}$$

Volume of the fluid (3D printing resin) exiting the syringe nozzle can be modelled in the following way,

$$V_n = \frac{\pi D_n^2}{4} * l_s$$

$$= \frac{\pi * 0.417^2}{4} * 100$$

$$V_n = \frac{17.3889}{4} \pi \qquad \text{(A.2)}$$

Using principle of volume conservation,

Setting the volume of fluid (3D printing resin) being pushed by the syringe plunger equal to the volume of fluid (3D printing resin) exiting the syringe nozzle

$$\frac{(\pi D_s^2)}{4} * h_f = \frac{\pi D_n^2}{4} * l_s$$

$$\Rightarrow \frac{68.0625}{4} \pi h_f = \frac{17.3889}{4} \pi$$

Hence, the Feed rate for (D_n = 417μm) is h_f = 0.26mm

Similarly, the feed values (amount of resin displaced by the plunger) can be calculated depending upon the value of the nozzle diameter supplied.

A.2 Evaluation of expected (theoretical) width of the strand in term of speed of plunger and print head.

Volume of the resin displaced by the plunger is equal to the volume of the resin exiting the nozzle

$$\pi \frac{\mathrm{D}_s^2}{4} \mathrm{h_f} = \pi \frac{{w_s}^2}{4} l_s$$

$$\mathrm{D}_s^2 \mathrm{h_f} = {w_s}^2 l_s \tag{A.3}$$

Where, D_s is the internal diameter of the syringe (mm), $\mathrm{h_f}$ is the feed (amount of plunger movement) (mm), w_s is the expected width of the strand (microns) and l_s is the length of the strand in mm.

Differentiating both sides of equation (A.3) with respect to time t, we get,

$$D_s^2 \frac{dh_f}{dt} + 2 D_s h_f \frac{dD_s}{dt} = {w_s}^2 \frac{dl_s}{dt} + 2\, w_s l_s \frac{d\, w_s}{dt} \tag{A.4}$$

Here, $\frac{\mathrm{dh_f}}{\mathrm{dt}}$ is the plunger speed (mm/min) which can be represented as $\mathrm{v_p}$

$\frac{\mathrm{d}D_s}{\mathrm{dt}}$ is zero because internal diameter of the syringe and will be constant

$\frac{\mathrm{d}l_s}{\mathrm{dt}}$ is the printer head speed (mm/min) which can be represented as $\mathrm{v_H}$

$\frac{\mathrm{d}w_s}{\mathrm{dt}}$ is zero because the width of the strand for a particular run is assumed to be constant and is not dependent on time t.

Therefore, Equation (A.4) reduces to,

$$D_s^2 \frac{dh_f}{dt} = \ w_s{}^2 \ \frac{dl_s}{dt} \tag{A.5}$$

$$v_p = \ w_s{}^2 \ v_H$$

$$w_s = D_s \sqrt{\frac{v_p}{v_H}} \tag{A.6}$$

Plunger speed (mm/min) can be equated in the following way

$$v_p = \frac{h_f}{t_1} \tag{A.7}$$

Where, h_f is the distance moved by the plunger(mm) and t_1 is the time taken (min)

Print head speed (mm/min) can be equated in the following way

$$v_H = \frac{l_s}{t_2} \tag{A.8}$$

Where, l_s is the distance moved by the print head (mm) and t_2 is the time taken (min)

The time taken by the plunger to travel a certain distance and the time taken by the print head to move from one position to another position will be equal, since both the motions are coordinated.

$$t_1 = \ t_2$$

Therefore,

Where t_1 is the time taken by the plunger to travel a certain distance and t_2 is the time taken by print head to move from one position to another

Therefore,

$$w_s = D_s \sqrt{\frac{\mathrm{h_f}}{l_s}} \tag{A.9}$$

A.3 Analysis of feed for Strands considered as parallelepiped and segment of circle profile

1) Volume of Strand fabricated considering a cuboid or parallelepiped profile (Initial Assumption).

Volume of the Strand = length ($\mathrm{l_s}$) x width ($\mathrm{w_s}$) x height ($\mathrm{h_s}$)

Where, $\mathrm{l_s}$ is the length of the strand fabricated (equal to 100mm), $\mathrm{w_s}$ is the Nozzle diameter (equal to 0.417mm) and $\mathrm{h_s}$ is the Nozzle-to-bed distance (equal to 0.100mm)

Therefore, volume (V) of the strand fabricated is $\mathrm{l_s}$ x $\mathrm{w_s}$ x $\mathrm{h_s}$

$$\mathrm{Vp} = 100 \times 0.417 \times 0.100 = 4.17\mathrm{mm}^3 \tag{A.10}$$

2) Volume of Strand fabricated considering a circle profile (observed profile)

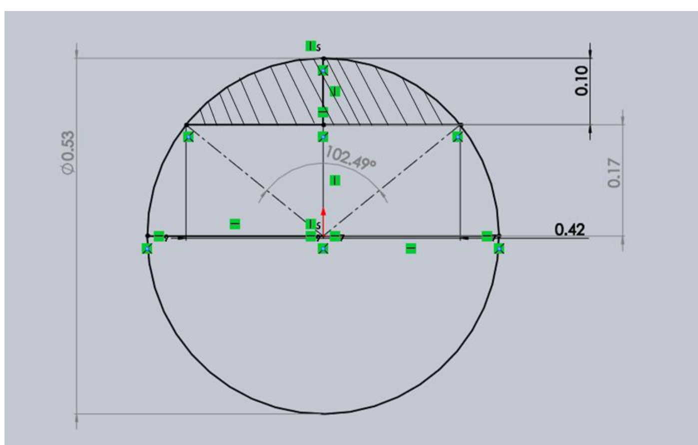

Figure A.2 Photo-Polymerized strand having a segment of a circle profile

Volume of the Strand fabricated (Volume of the shaded portion extruded out) is equal to area of the Segment of the circle times the extruded length

Where the area of the segment is equal to area of the sector minus the area of the triangle

$$A_{segment} = A_{sector} - A_{triangle}$$

Area of the sector of the circle, $A_{sector} = \frac{n^{\circ}}{360^{\circ}} \pi r^2 = \frac{102.49^{\circ}}{360^{\circ}} \pi \ (\frac{0.53}{2})^2 = 0.06mm^2$

Area of the triangle, $A_{triangle} = \frac{1}{2}$ x base x altitude = $\frac{1}{2}$ x 0.417 x 0.17 = $0.035mm^2$

Therefore, Area of the segment = 0.06 – 0.035 = $0.025mm^2$

Hence, the volume of the strand fabricated is equal to Area of the segment of the circle times the extruded length,

$V_c = 0.025 \text{ x } 100 = 2.5mm^3$ (A.11)

3) Calculation of the Feed (based on cuboid profile):

Volume of the resin displaced by the plunger = Volume of the Strand fabricated (cuboid profile)

Therefore, $\pi \ (\frac{8.25}{2})^2 \ f = 4.17$ [from equation (A.10)]

Or, f = 0.078mm = 78μm

Hence the feed associated with parallelepiped profile for 417μm nozzle is 78μm.

4) Calculation of the Feed (based on segment of circle profile):

Volume of the resin displaced by the plunger is equal to the volume of the Strand fabricated (segment of circle profile)

Therefore, $\pi \ \left(\frac{8.25}{2}\right)^2 \ f = 2.5$ [from equation (A.11)]

Or, f = 0.047mm = 47μm

Hence the feed associated with segment of a circle profile for 417μm nozzle is 47μm

The difference in feed (cuboid and segment of circle profile) is

Δf = 78 – 47 = 31 μm

Similar calculation can be performed based on the nozzle diameter and the nozzle-to-bed distance considered.

APPENDIX B

HISTROICAL ACHIEVMENTS IN 3D PRINTING

The table in Appendix B list the extensive historical achievements in the industry of 3D printing. This table is the continuation of Table 1.1 [4].

Date	Achievement	Name of the Achiever
1987	Development of Stereolithography (SLA)	3D Systems
1988	Development of SL material ,DuPont's Somos Stereolithography machine and commercialization of first generation acrylate resin	Partnership between 3D systems and Ciba-Geigy
1990	Invented Stereos Stereolithography system	Electro Optical System (EOS) of Germany
1990	Mark 1000 SL system for visible light resin	Quadrax
1991	Invention of Fused Deposition Modelling (FDM)	Stratasys
1991	Solid Ground Curing (SCG)	Cubital
1991	Laminated Object Manufacturing (LOM)	Helisys
1992	Selective Laser Sintering (SLS)	DTM (now a part of 3D Systems)
1992	Soliform Stereolithography system	Teijin Seiki
1992	Vinyl ether Exactomer resin products for SL	Allied Signal
1993	Direct Shell Product Casting (DSPC)	Soligen

1994	Invention of ModelMaker	Solidscape
1996	Invention of Genisys machine	Stratatsys
1996	Launch of Z402 3D printer	Z Corporation
1999	Invention of Thermojet	3D Systems
2000	Development of Quadra, a 3D inkjet printer	Objet geometries of Israel
2000	Introduction of Prodigy, a machine that produces parts using ABS plastics	Stratatsys
2001	Introduction of desktop machine that laminates thin sheets of PVC plastic	Solido of Israel
2001	Introduction of Z810 system	Z Corporation
2001	Launch of EOSINT 380, a laser-sintering machine	EOS Corporation
2002	Introduction of Dimensional 3D printer	Stratatsys
2003	ZPrinter 310 system	Z Corporation
2003	T612 system for making wax patterns for investment castings	Solidscape
2003	EOSINT M 270 direct metal laser- sintering machine	EOS
2004	Introduction of “Triplets”	Stratatsys

2004	Vanquish photopolymer-based system	Envisiontec
2004	Launch of small RX-1 metal-based machine	ProMetal division of Ex One
2004	Launch of T66 Benchtop and T612 Benchtop systems	Solidscape
2005	Launch of Spectrum Z510, a colour 3D-printing system	Z Corporation
2005	Launch of Sinterstation Pro, a large-frame laser-sintering machine	3D Systems
2005	Introduction of Eden500V, a large-format PolyJet 3D printer	Object Geometries
2005	Launch of SLM ReaLizer 100 selective laser-melting machine	MTT Technologies Group
2006	Launch of InVision DP (dental professional) system that includes an InVision 3D printer and 3D scanner for the dental market	3D Systems
2006	Introduction of Dimension 1200 BST and SST systems	Stratatsys
2006	Launch of ZScanner 700 handheld 3D scanner	Z Corporation

2006	Launch of the EOSINT P 390, EOSINT P 730 and Formiga P 100 laser-sintering system	EOS
2007	Launch of V-Flash 3D printer	3D Systems
2007	Introduction of ZPrinter 450	Z Corporation
2007	Introduced multi-material Connex500 3D-printing system.	Objet Geometries
2008	Introduced a biocompatible FDM material, ABS-M30i	Stratasys
2008	Launched high-elongation polyamide PrimePart DC for plastic laser sintering	EOS of Germany
2008	Launch of a larger selective laser-melting machine, the SLM 250-300	England, MTT
2008	Introduced a vapour-honing product called Fortus Finishing Stations for finishing FDM parts made in ABS	Stratasys
2009	Released the RapMan 3D printer kit based on the RepRap open-source system	Bits from Bytes of England
2009	Launch of Dimatix Materials Printer DMP-3000	Fujifilm Dimatix
2009	Introduced automated monochrome ZPrinter 350	Z Corporation

2009	Launch of two new plastic laser- sintering machines: the EOSINT P 395 and EOSINT P 760. The large-frame P 760 machine	EOS
2010	Launch of extrusion-based portable personal UP! 3D printer	Delta Micro Factory Corp.
2010	Introduced the monochrome ZPrinter and the color ZPrinter 250	Z Corporation
2010	Launch of Objet24 3D printer	Objet
2011	Launch of Objet260 Connex 3D printer	Objet
2011	Launch of a new crossover AM machine, the Fortus 250mc, which runs the ABSplus material with a soluble support material	Stratasys
2012	Launch of MakerBot Replicator	Makerbot
2012	Launch of MAGIC LF600 large-frame AM machine	EasyClad (France)
2012	Launch of second-generation machine	Soliddoodle
2012	Launch of Mojo 3D printer	Stratasys
2012	Launch of Objet30 Pro	Objet (Israel)
2012	Introduced laser- based vat Photo-Polymerization system	Formlabs
2012	Launch of Objet1000 system	Object

2012	Launch of first 3D bio-printing software	Orgonovo Holdings and Autodesk

APPENDIX C

NEA123T RESIN

The NEA123T (Norland Electronic Adhesive) [18] resin could be adopted for characterization of PP process due to their better dimensional stability in comparison with Solarez resin. NEA123T is a Non-Newtonian time depended fluid which has shear thinning behaviour, which implies that the viscosity increases with the decrease in shear rate. It has thixotropic behaviour in which the viscosity decreases over time when shaken or stressed (time dependent viscosity). NEA123T resin is a high viscosity resin having a viscosity between 300,000 – 400,000 cps depending upon the shear rate. The curing time for a layer of NEA123T dispersed onto a build platform is 5-10 seconds depending upon the UV intensity. The NEA123T is an extremely stable resin even when not exposed to UV light. This stability is due to its high viscosity.

The NEA123T resin has peak sensitivity when exposed to UV light emitted at a wavelength of 365nm [18]. The NEA123T has a heat catalyst mixed into the resin and heat treatment can also be used for curing the resin but the polymerization time is slower when compared to the UV curing process. It takes about three hours at 80°C and 10 minutes when heated at 125°C in a convention oven although faster curing time is possible in an infrared oven. Any temperature below 60°C will not initiate the PP process.

REFERENCES

[1] H. Kodama, A Scheme for Three-Dimensional Display by Automatic Fabrication of Three-Dimensional Model, Vols. J64-C, No.4, IEICE TRANSACTIONS on Electronics (Japanese Edition), 1981.

[2] H. Kodama, Automatic method for fabricating a three-dimensional plastic model with photo-hardening polymer, Vols. 52, No. 11, Review of Scientific Instruments, 1981.

[3] C. W. Hull, "Apparatus for production of three-dimensional objects by Stereolithography". Patent US 4575330 A, 11 March 1986.

[4] T. W. a. T. Gornet, "History of Additive Manufacturing," Wohlers Report , 2014.

[5] C. C. Kai, K. F. Leong and C. S. Lim, Rapid Prototyping, World Scientific, 2003.

[6] D. World, "What do you know about the eight additive manufacturing processes," 2015. [Online]. Available: http://www.designworldonline.com/.

[7] "3D printing from scratch," [Online]. Available: http://3dprintingfromscratch.com/common/3d-printer-filament-types-overview/.

[8] [Online]. Available: http://www.additive3d.com/photo.htm.

[9] Юкатан, "Polymerization of photopolymer by UV light," 2015.

[10] C. Hoyle, "Radiation Curing of Polymeric Materials," Am. Chem. Soc., Washington, DC, 1990.

[11] A. Ravve, "Light-Associated Reactions of Synthetic Polymers," Springer Science+Business Media, LLC., New York, 2006.

[12] J. P. Fouassier, " Photoinitiators for Polymer Synthesis: Scope, Reactivity and Efficiency," Weinheim, Germany: Wiley-VCH Verlag GmbH & Co. KGaA, 2012.

[13] J. Fouassier, X. Allonas and D. Burget, Photo-Polymerization reactions under visible lights: principle, mechanisms and examples of applications, 2003.

[14] Materialgeeza, "Stereolithograthy apparatus schematic".

[15] "Pinshape Blog," [Online]. Available: https://blog.pinshape.com/fdm-vs-sla-kudo3d-explains-3d-printer-tech/.

[16] "Nikon," [Online]. Available: http://www.nikon.com/.

[17] P. Ravi, P. S. Shiakolas, J. Oberg, A. Batra and S. Faizee, "On the Development of a modular 3d Bio-Printer for research in biomedical device fabrication," American Society of Mechanical Engineers (ASME), 2015.

[18] "NEA123T ultraviolet and heat curable polymer resin," Norland Products, [Online]. Available: : https://www.norlandprod.com/adhesives/nea%20123t.html.

[19] "UV15DC80 primary ultraviolet and secondary heat curable polymer resin.," Master Bond, [Online]. Available: http://www.masterbond.com/tds/uv15dc80.

[20] A. Ranellucci, *Slic3r V1.7.1*.

[21] RepRapDiscount.com, "Reprap Universal Mega Board with Allegro driver," [Online].

[22] Solarez, "Solarez 3D printing resin Source," [Online]. Available: http://solarez.com/products/solarez-3-d-printing-resin-medium-viscosity-quart/.

[23] "Viscosity of fluids," [Online]. Available: http://www.research-equipment.com/viscosity%20chart.html.

[24] Bivar, "Bivar Ultraviolet Light Emitting Diodes (LEDs)," [Online]. Available: http://www.bivar.com/led-indication/leds/ultraviolet-leds/3mm-through-hole.

[25] "Stepper motor part no. 28F47-2.1-906," Haydon Switch instruments, [Online]. Available: http://www.haydonkerk.com/.

[26] L. L. L. a. D. T. R D Farahani, "Processing parameters investigation for the fabrication of self-supported and freeform polymeric microstructures using ultraviolet-assisted three-dimensional printing," 2014.

[27] N. Products, "NEA123MB resin," [Online]. Available: https://www.norlandprod.com/adhesives/nea%20123.html.

[28] R. S. G. Taylor, Comprehensive system-level optimization of thermoelectric devices for electronic cooling applications, Components and Packaging Technologies, Vols. Volume:31, Issue: 1, IEEE.

[29] Tellurex, "Frequently asked questions about our product," [Online]. Available: http://tellurex.com/.

[30] "LabVIEW," [Online]. Available: http://www.ni.com/labview/.

[31] "FDM Extruders," 2014.

[32] N. Gada, M. Aliakbar, H. Lohawala, A. Peiris and S. Gutierrez, "3D Bio-Printer Dispenser Head," 2015.

[33] H.-W. G. &. C. KG, *Repetier-Host V1.0.6.*

BIOGRAPHICAL INFORMATION

Shahid Faizee has earned his Bachelor of Engineering Degree from Manipal University, Manipal, India in May 2012. He then worked in Cycloid Systems as an Application Engineer during the term 2012-2013. He then joined University of Texas at Arlington to pursue his Master of Science degree in Mechanical Engineering in fall 2013 and obtained the degree in fall 2015. His research interest includes 3D printing, additive manufacturing technology and Control Systems.